arXiv:hep-ph/0206012v1 3 Jun 2002

COULOMB INTERFERENCE IN HIGH-ENERGY pp AND $\bar{p}p$ SCATTERING.

V. A. PETROV[a,1], E. PREDAZZI[b,2] and A. PROKUDIN[a,b,3]

(a) Institute For High Energy Physics,
142281 Protvino, RUSSIA

(b) Dipartimento di Fisica Teorica,
Università Degli Studi Di Torino,
Via Pietro Giuria 1, 10125 Torino,
ITALY
and
Sezione INFN di Torino,
ITALY

An analysis of the Coulombic amplitude and its interference with the nuclear amplitude which is driven by the three-component Pomeron [1] is presented. It is shown that different approaches towards the Coulomb phase evaluation give approximately uniform result at all energies and the difference is negligible at **RHIC** and **LHC** energies. We show that the use of the amplitude which was fitted to accomodate nucleon data only (in the region $0.01 \leq |t| \leq 14.5$ (GeV^2)) combined with the Coulomb amplitude, reproduces the existing data in the Coulomb interference domain quite accurately without any adjustement of the parameters. As a consequence, we predict the differential cross section in the region of the Coulomb nucleon interference for both **RHIC** and **LHC** energies.

1 INTRODUCTION

In Ref. [1] an eikonal model of a three-component Pomeron has been suggested and successfully used for describing the high energy pp nad $\bar{p}p$ data in the region of large momentum transfer $0.01 \leq |t| \leq 14.5$ (GeV^2) . In this paper we apply the model to the region of small momentum transfer $0 \leq |t| \leq 0.01$ (GeV^2).

[1] *E-mail: petrov@mx.ihep.su*
[2] *E-mail: predazzi@to.infn.it*
[3] *E-mail: prokudin@to.infn.it*

The problem is a proper account of the Coulomb interaction which is most important at the smallest $|t|$. The standard way to do this is to represent the whole scattering amplitude $T(s,t)$ which is dominated by the Coulomb force at low momentum transfer and by the hadronic force at higher momentum transfer as

$$T(s,t) = T^N(s,t) + e^{i\alpha\Phi}T^C(s,t), \tag{1}$$

where if we normalize the scattering amplitude so that

$$\frac{d\sigma}{dt} = \frac{|T(s,t)|^2}{16\pi s^2}, \tag{2}$$

the Born Coulomb amplitude for pp and $\bar{p}p$ scattering is

$$T^C(s,t) = \mp\frac{8\pi\alpha s}{|t|}. \tag{3}$$

The upper (lower) sign corresponds to the scattering of particles with the same (opposite) charges. $T^N(s,t)$ stands for purely strong interaction amplitude, and the phase Φ depends generally on energy, the momentum trasfer and on the properties of T^N. The study of the Coulomb nuclear interference is very important for extracting the real part of the strong interaction amplitude.

The issue of Coulombic amplitude and its interference with the nuclear component was addressed in many papers in the past. West and Yennie [2] examined the Coulomb-nuclear interference using Feynman diagrams. R. Cahn [3] considered the same task in the framework of the Eikonal model; his results were quite convincing (though the modifications were very small compared to [2]) and proved that the Eikonal model is a very convenient basis for analyzing the Coulomb-nuclear interference.

The Coulombic phase has atracted the attention of many authors. Using the WKB approach in potential theory, Bethe [4] derived, for proton-nucleus scattering, the expression

$$\Phi = 2\ln(1.06/|\mathbf{k_1}|b\Theta), \tag{4}$$

where $|\mathbf{k_1}|$ is the c.m. momentum, b is the range of strong-interaction forces defined by the size of the nucleus, and Θ the c.m. scattering angle. Similar results were derived within potential theory by several authors [5], [6].

A relativistic derivation of the phase was attempted by Soloviev [7], who obtained

$$\Phi = 2\ln(2/\Theta), \tag{5}$$

a result which differs considerably from the result of Bethe [4]. Utilizing the same technique, Rix and Thaler [8] derived a result quantitevely close to that of Bethe [4].

West and Yennie [2], as already mentioned, obtained the phase of Coulomb-nuclear interference using Feynman diagrams. For a conventional parametrization $T^N(s,t) \sim exp(-B|t|/2)$, the result of West and Yennie [2] reads

$$\Phi_{W-Y} = \mp\Big[\ln(B|t|/2) + \gamma + O(B|t|)\Big], \tag{6}$$

where $\gamma = 0.577...$ is Euler's constant. The upper (lower) sign corresponds to the scattering of pp ($\bar{p}p$).

Cahn [3] analized also the effect of the electromagnetic form factor and obtained a general expression for the phase. The results of [3] were in complete agreement with [2] and especially the formula (6) was derived from a rather different perspective.

The main difference from the result [2] is a shift of the Coulomb amplitude due to the form factor's influence on the phase. If we introduce the electromagnetic form factor of the proton, the Born term of the Coulomb amplitude has the following form

$$T^C(s,t) = \mp\frac{8\pi\alpha s}{|t|} f^2(|t|), \tag{7}$$

where the form factor may be chosen as

$$f(|t|) = e^{-2|t|/\Lambda^2}, \;\; \Lambda^2 = 0.71\ GeV^2. \tag{8}$$

In this case the Coulomb phase has the following form

$$\Phi_{Cahn} = \mp\Big[\ln\Big(\frac{B|t|}{2}\Big) + \gamma + \ln\Big(1 + \frac{8}{B\Lambda^2}\Big) + (4|t|/\Lambda^2)\ln(4|t|/\Lambda^2) + 2|t|/\Lambda^2\Big]. \tag{9}$$

All these results were obtained under the assumption that $|t| \to 0$. The derivation of the phase in a large domain of momentum transfer was attempted by Selyugin [9], and Kopeliovich and Tarasov [12]. In the region

of interest for the present paper $0 \leq |t| \leq 0.01\ GeV^2$, the latter results are similar to that of Cahn [3] and the main difference is in the dip region of the differential cross-sections. The phase obtained in [9] accurately takes into account the dipole form factor

$$f(|t|) = \Big[\frac{\Lambda^2}{\Lambda^2 + |t|}\Big]^2, \quad \Lambda^2 = 0.71\ GeV^2, \tag{10}$$

and the complicated structure of the nucleon amplitude.

The phase has the following form

$$\Phi_{Selyugin} = \mp\Big[\ln\frac{|t|}{4} + 2\gamma - \nu_s - i\frac{8\pi s}{T_N(s,t)}\int_0^\infty bdbJ_0(b\sqrt{-t})\delta_C(s,b)\cdot \Big(e^{2i\delta_N(s,b)} - 1\Big)\Big],$$

where

$$\nu_s = 0.11\log(1 + 400|t|) \tag{11}$$

takes into account influence of the form factor on the pure coulombic phase, and

$$\delta_C(s,b) = \ln b + K_0(b\Lambda) + \frac{11}{12}b\Lambda K_1(b\Lambda) + \frac{5}{24}b^2\Lambda^2 K_0(b\Lambda) + \frac{1}{48}b^3\Lambda^3 K_1(b\Lambda). \tag{12}$$

The prescription of West and Yennie [2] was successfully used by several authors [10] and [11] for describing differential cross sections in low t region.

In what follows we will investigate four different cases of the Coulomb phase – the phase calculated with the nucleon amplitude of the model [1] (which does not acquire any additional parameter) with the prescription of West and Yennie [2], the phase calculated with prescription of Cahn [3], the prescription of Selyugin [9], and the phase equal to zero.

2 THE NUCLEAR AMPLITUDE

We believe that any nuclear amplitude that is capable of a high accuracy description of the combined set of high energy pp and $\bar{p}p$ data (total and differential cross sections, ρ parameter etc.) over the entire $|t|$ spectrum, if properly combined with the correct Coulomb amplitude *must* account well

for the data in the interference region. That this is so, we will prove using the particular nuclear amplitude which has been derived in [1] to describe total and differential cross sections at high energies ($\sqrt{s} \geq 10GeV$) in the range of momentum transfer $0.01 < |t| < 14.5\ GeV^2$ using the eikonal approach (another one could have been the amplitude of [13]). We just write the nuclear amplitude of [1]

$$T(s,\vec{b}) = \frac{e^{2i\delta(s,\vec{b})} - 1}{2i}\ , \tag{13}$$

where the eikonal has the following form

$$\delta_{pp}^{\bar{p}p}(s,b) = \delta_{\mathbb{P}_1}^{+}(s,b) + \delta_{\mathbb{P}_2}^{+}(s,b) + \delta_{\mathbb{P}_3}^{+}(s,b) \mp \delta_{\mathbb{O}}^{-}(s,b) + \delta_{f}^{+}(s,b) \mp \delta_{\omega}^{-}(s,b). \tag{14}$$

We refer the reader to the original literature for details; let us simply recall that here $\delta_{\mathbb{P}_{1,2,3}}^{+}(s,b)$ are Pomeron contributions. The superscript '+' denotes C even trajectories (the Pomeron trajectories have quantum numbers 0^+J^{++}), while '$-$' denotes C odd trajectories. $\delta_{\mathbb{O}}^{-}(s,b)$ is the Odderon contribution (i.e. the C odd partner of the Pomeron whose quantum numbers are 0^-J^{--}); δ_{f}^{+} and $\delta_{\omega}^{-}(s,b)$ are the contributions of secondary Reggeons, (f as representative of the $C=+1$ families and ω of the $C=-1$).

In order to relate t- and b-spaces one proceeds via Fourier-Bessel transforms

$$\begin{aligned} \hat{f}(t) &= 4\pi s \int_0^\infty db^2 J_0(b\sqrt{-t}) f(b)\ , \\ f(b) &= \frac{1}{16\pi s} \int_{-\infty}^0 dt J_0(b\sqrt{-t}) \hat{f}(t)\ . \end{aligned} \tag{15}$$

Using this parametrisation we obtain the following expressions for the Coulomb phase

$$\Phi_{W-Y} = \mp \frac{\sum_i \delta_i(s,t=0)\Big[\ln\left(\frac{\rho_i(s)|t|}{4}\right) + \gamma\Big]}{\sum_i \delta_i(s,t=0)}, \tag{16}$$

and

$$\begin{aligned} \Phi_{Cahn} = \mp \frac{\sum_i \delta_i(s,t=0)\Big[\ln\left(\frac{\rho_i(s)|t|}{4}\right) + \gamma + \ln\left(1+\frac{16}{\rho_i(s)\Lambda^2}\right)\Big]}{\sum_i \delta_i(s,t=0)} \\ \mp(4|t|/\Lambda^2)\ln(4|t|/\Lambda^2) \mp 2|t|/\Lambda^2, \end{aligned} \tag{17}$$

where $\rho_i^2 = 4\alpha_i'(0)\ln s/s_0 + r_i^2$, $i = P_1, P_2, P_3, O, f, \omega$. The upper (lower) signs correspond to pp ($\bar{p}p$).

Crossing symmetry is restored by replacing $s \to se^{-i\pi/2}$. We introduce the dimensionless variable

$$\tilde{s} = \frac{s}{s_0} e^{-i\frac{\pi}{2}} \ , \tag{18}$$

in terms of which we give each $C+$ and $C-$ contribution with its appropriate signature factor in the form

$$\delta^+(s,b) = i\frac{c}{s_0}\tilde{s}^{\alpha(0)-1}\frac{e^{-\frac{b^2}{\rho^2}}}{4\pi\rho^2} \ , \tag{19}$$
$$\rho^2 = 4\alpha'(0)\ln\tilde{s} + r^2 \ ,$$
$$(C = +1) \ ;$$
$$\delta^-(s,b) = \frac{c}{s_0}\tilde{s}^{\alpha(0)-1}\frac{e^{-\frac{b^2}{\rho^2}}}{4\pi\rho^2} \ , \tag{20}$$
$$\rho^2 = 4\alpha'(0)\ln\tilde{s} + r^2 \ ,$$
$$(C = -1) \ .$$

3 RESULTS

In [1], the adjustable parameters have been fitted over a set of 982 pp and $\bar{p}p$ data[4] of both forward observables (total cross-sections σ_{tot}, and ρ – ratios of real to imaginary part of the amplitude) in the range $8. \leq \sqrt{s} \leq 1800.\ GeV$ and angular distributions ($\frac{d\sigma}{dt}$) in the ranges $23. \leq \sqrt{s} \leq 1800.\ GeV$, $0.01 \leq |t| \leq 14.\ GeV^2$. A good $\chi^2/d.o.f. = 2.60$ was obtained and the parameters are given in Table 1.

[4]The data are available at
REACTION DATA Database *http://durpdg.dur.ac.uk/hepdata/reac.html*
CROSS SECTIONS PPDS database *http://wwwppds.ihep.su:8001/c5-5A.html*
http://pdg.lbl.gov/2000/contents_plots.html

	Pomeron$_1$		**f-Reggeon**
$\Delta_{\mathbb{P}_1}$	0.0578 ± 0.0020	Δ_f	-0.31 (FIXED)
$c_{\mathbb{P}_1}$	53.007 ± 0.795	c_f	191.69 ± 2.12
$\alpha'_{\mathbb{P}_1}$	0.5596 ± 0.0078 (GeV^{-2})	α'_f	0.84 (GeV^{-2}) (FIXED)
$r^2_{\mathbb{P}_1}$	6.3096 ± 0.2522 (GeV^{-2})	r^2_f	31.593 ± 1.099 (GeV^{-2})
	Pomeron$_2$		**ω-Reggeon**
$\Delta_{\mathbb{P}_2}$	0.1669 ± 0.0012	Δ_ω	-0.53 (FIXED)
$c_{\mathbb{P}_2}$	9.6762 ± 0.1600	c_ω	-174.18 ± 2.72
$\alpha'_{\mathbb{P}_2}$	0.2733 ± 0.0056 (GeV^{-2})	α'_ω	0.93 (GeV^{-2}) (FIXED)
$r^2_{\mathbb{P}_2}$	3.1097 ± 0.1817 (GeV^{-2})	r^2_ω	7.467 ± 1.083 (GeV^{-2})
	Pomeron$_3$		
$\Delta_{\mathbb{P}_3}$	0.2032 ± 0.0041	s_0	1.0 (GeV^2) (FIXED)
$c_{\mathbb{P}_3}$	1.6654 ± 0.0669		
$\alpha'_{\mathbb{P}_3}$	0.0937 ± 0.0029 (GeV^{-2})		
$r^2_{\mathbb{P}_3}$	2.4771 ± 0.0964 (GeV^{-2})		
	Odderon		
$\Delta_{\mathbb{O}}$	0.19200 ± 0.0025		
$c_{\mathbb{O}}$	0.0166 ± 0.0022		
$\alpha'_{\mathbb{O}}$	0.048 ± 0.0027 (GeV^{-2})		
$r^2_{\mathbb{O}}$	0.1398 ± 0.0570 (GeV^{-2})		

Table 1: Parameters obtained in [1].

We now consider the complete set of data including the Coulomb region which consists of 2158 data[5]. To these data, we apply the model including the Coulomb part with its phase and we simply plot the physical quantities without any additional fitting.

The total cross sections and the ratios of real to imaginary parts of the forward amplitude are presented in Figs. 1 and 2.

[5]The data are available at
REACTION DATA Database *http://durpdg.dur.ac.uk/hepdata/reac.html*
CROSS SECTIONS PPDS database *http://wwwppds.ihep.su:8001/c5-5A.html*
http://pdg.lbl.gov/2000/contents_plots.html

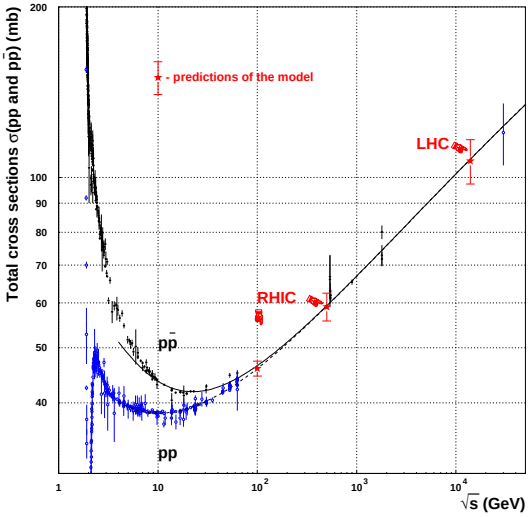

Figure 1: Total cross sections of pp scattering (hollow circles) and $\bar{p}p$ scattering (full circles) and corresponding curves in the model of Ref.[1].

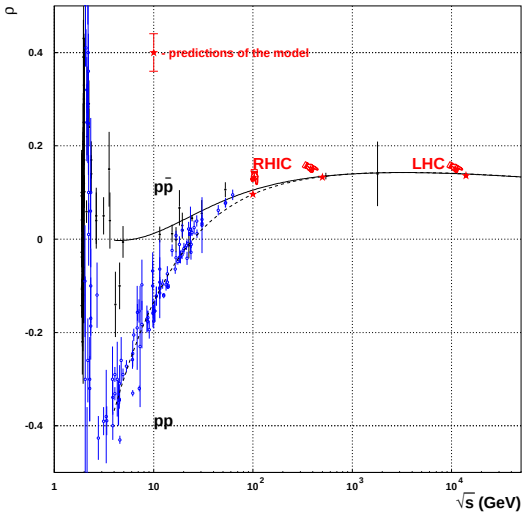

Figure 2: Ratios of the real to the imaginary part of the forward pp scattering amplitude (hollow circles) and $\bar{p}p$ scattering amplitude (full circles) and corresponding curves in the model of Ref. [1].

In order to compare different approaches to the Coulomb phase, we have calculated the χ^2 for the region of low $|t|$: $0 \leq |t| \leq 0.01$ (GeV^2) in four different cases:

1. The Coulomb phase is equal to zero.
2. The Coulomb phase is calculated with the prescription of West and Yennie (16).
3. The Coulomb phase is calculated with the prescription of Cahn (17).
4. The Coulomb phase is calculated with the prescription of Selyugin (11).

The results may be found in Table 2.

Coulomb phase	Number of points	χ^2 per point
$\Phi = 0$	604	3.49
Φ_{W-Y} (16)	604	2.09
$\Phi_{Cahn}(17)$	604	1.86
$\Phi_{Selyugin}(11)$	604	1.84

Table 2: χ^2 per point for the region of low $|t|$: $0 \leq |t| \leq 0.01\ (GeV^2)$.

As is seen from the Table 2, the experimental data marginally "prefer" the Coulomb phase calculated with the prescription of Cahn [3] and Selyugin [9] over that of West and Yennie but taking the Coulomb phase equal to zero is excluded by the data and this is gratifying on physical grounds. The difference between the phases of [3] and [9] is negligible in the small $|t|$ region of the interest (as may be seen in Fig. 3), though the exact result obtained in [9] over the whole kinematical region of $|t|$ shows that the difference is drastic in the region of the diffractive dip (as seen in Fig. 4).

Apart from this, the Coulomb phase calculated in the Selyugin approach exhibits a non trivial behaviour of the real part (which has a zero in the point of the diffractive dip), and of the imaginary part (which has a minimun in the same point) Fig. 4.

The diffrence between the approaches of Cahn [3] and of West and Yennie [2] is more pronounced even in the region of low t as may be seen in Fig. 3.

It is of some interest to perform a more detailed comparison of the χ^2 derived for the region of low momemtun transfer. This can be found in Table 3 for Φ_{W-Y}, Φ_{Cahn}, and $\Phi_{Selyugin}$.

With all due caution, a general pattern emerges; some data points have anomalously large χ^2 values and these are the same in all cases.

The $\bar{p}p$ differential cross section at $\sqrt{s} = 546\ GeV$, for instance, sticks out conspicuously. The explanation is the normalisation of the cross section. The sysytematical error allows to change the normalisation of the data in the $\pm 10\%$ corridor. If we could multiply our predictions by a factor 1.06, we would have a good description of this set of data, as is seen in Fig. 5 and 6.

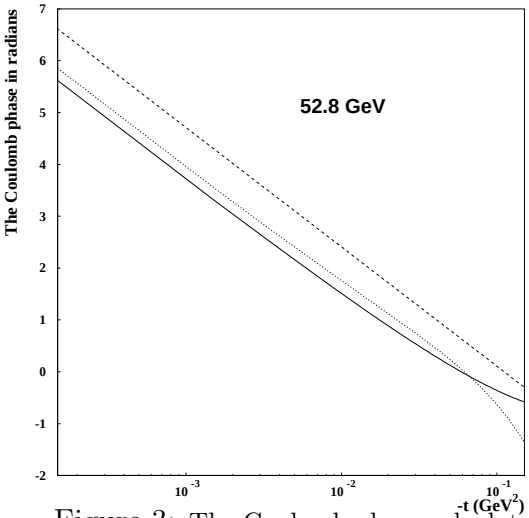

Figure 3: The Coulomb phase calculated in the framework of Selyugin [9] (the solid line) and of Cahn [3] (the dotted line) and of West and Yennie [2] (the dashed line) in the region of small t. $\sqrt{s} = 52.8\ GeV$

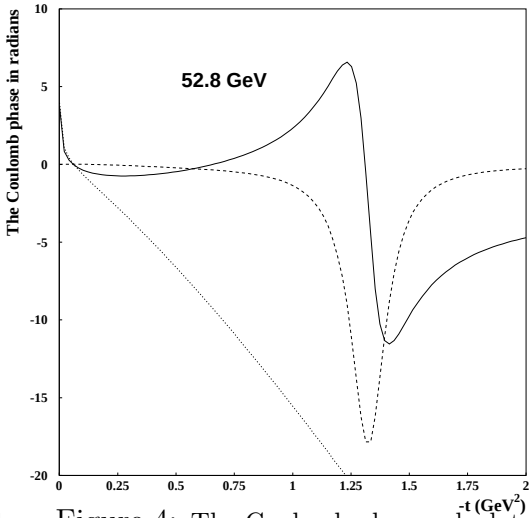

Figure 4: The Coulomb phase calculated in the framework of Selyugin [9] , real part (the solid line) and imaginary part (the dashed line) and in that of Cahn [3] (the dotted line) in the region of high t.

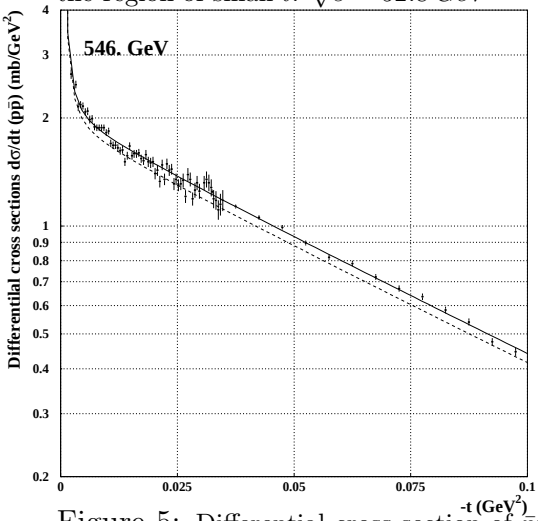

Figure 5: Differential cross section of $\bar{p}p$ scattering and curves corresponding to its description in the model. The dashed line represents our predictions. The solid curve is our predictions normalized by a factor 1.06.

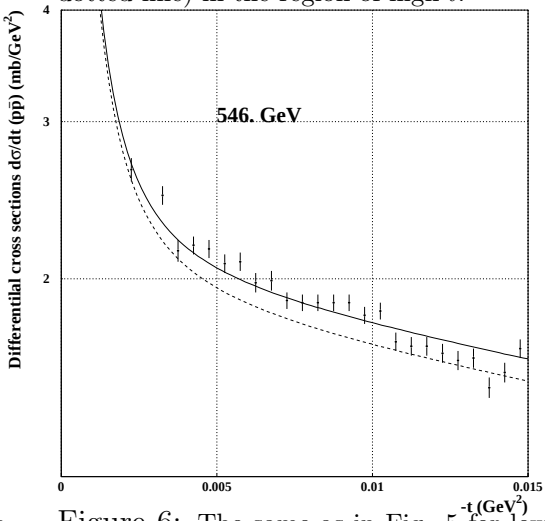

Figure 6: The same as in Fig. 5 for low t.

	Data	$\sqrt{s}\,(GeV)$	$0 \le \lvert t\rvert \le 0.01\,(GeV^2)$ **#points, ntot**	χ^2/ntot Φ_{W-Y}	χ^2/ntot Φ_{Cahn}	χ^2/ntot $\Phi_{Selyugin}$
1	$\sigma_{total}^{\bar{p}p}$		33	0.7167	0.7167	0.7167
2	σ_{total}^{pp}		68	0.3617	0.3617	0.3617
3	$\rho^{\bar{p}p}$		11	0.6086	0.6086	0.6086
4	ρ^{pp}		48	0.4326	0.4326	0.4326
5	$\frac{d\sigma}{dt}^{\bar{p}p}$	24.3	26	1.4965	2.4879	2.8105
6	$\frac{d\sigma}{dt}^{\bar{p}p}$	30.4	21	1.4702	1.4130	1.4027
7	$\frac{d\sigma}{dt}^{\bar{p}p}$	52.6	12	1.9847	1.4676	1.3440
8	$\frac{d\sigma}{dt}^{\bar{p}p}$	62.3	3	1.0263	0.8135	0.7635
9	$\frac{d\sigma}{dt}^{\bar{p}p}$	541.0	37	2.0811	2.3993	2.5246
10	$\frac{d\sigma}{dt}^{\bar{p}p}$	546.0	15	11.4692	11.0364	10.9008
11	$\frac{d\sigma}{dt}^{pp}$	10.6	35	2.3342	2.0297	1.9610
12	$\frac{d\sigma}{dt}^{pp}$	12.3	37	1.5731	1.4169	1.3931
13	$\frac{d\sigma}{dt}^{pp}$	19.4	45	1.9674	1.7840	1.7509
14	$\frac{d\sigma}{dt}^{pp}$	22.2	45	1.4666	1.3374	1.3192
15	$\frac{d\sigma}{dt}^{pp}$	23.9	94	2.3910	2.3699	2.3087
16	$\frac{d\sigma}{dt}^{pp}$	24.3	25	1.1418	1.2638	1.3587
17	$\frac{d\sigma}{dt}^{pp}$	27.4	40	2.2246	2.0014	1.9607
18	$\frac{d\sigma}{dt}^{pp}$	30.7	8	0.3174	1.2071	1.5482
19	$\frac{d\sigma}{dt}^{pp}$	44.7	25	5.0147	2.9964	2.7679
20	$\frac{d\sigma}{dt}^{pp}$	52.8	21	7.1074	4.2590	3.9018
21	$\frac{d\sigma}{dt}^{pp}$	62.3	4	8.5177	6.7054	6.2988

Table 3: χ^2 per point for the region of low $|t|:\ 0 \le |t| \le 0.01\,(GeV^2)$ for Φ_{W-Y}, Φ_{Cahn}, and $\Phi_{Selyugin}$.

To appreciate the role of the Coulomb phase, we plot the angular distributions with the appropriate Coulomb phase and with the phase taken equal to zero in the following figures 7, 8. Even though the difference is minimal, the numerical conclusion is that the data, quite unambiguously, prefer the appropriate nonzero Coulomb phase.

The comparison with the West-Yennie and Cahn phases is not shown because the plot would be undistinguishable from the Selyugin one.

Let us remind that no additional fitting was done.

We do not report here any of the pp and $\bar{p}p$ angular distributions which one obtains over the full range of $|t|$ values because the original reproduction

of these quantities is left basically unchanged by the Coulomb amplitude and the interested reader is referred to the original paper [1]. We simply report here, for completeness, the predictions at RHIC and LHC energies both in the interference region and over the entire $|t|$ range. Predictions of the model and comparison with the nuclear amplitude for **RHIC** and **LHC** are shown in figures 9, 10, 11, 12.

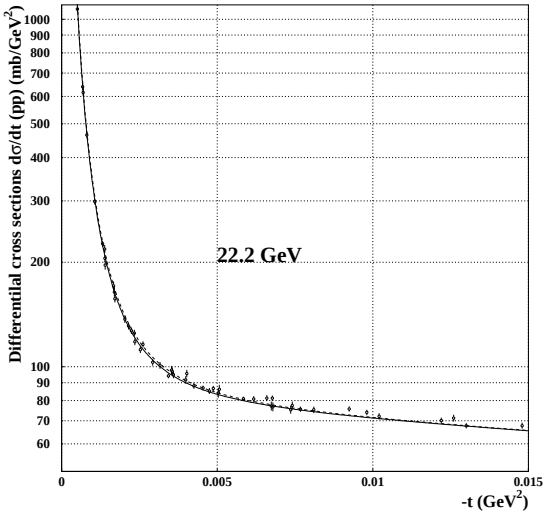

Figure 7: Differential cross section of pp scattering and curves corresponding to its description in the model. The solid line corresponds to the Coulomb phase calculated with prescription of Selyugin (11) and the dashed line corresponds to the zero phase.

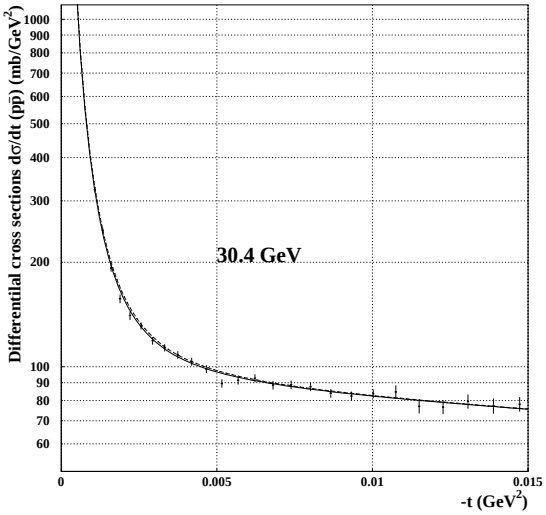

Figure 8: Differential cross section of $\bar{p}p$ scattering and curves corresponding to its description in the model. The solid line corresponds to the Coulomb phase calculated with prescription of Selyugin (11) and the dashed line corresponds to the zero phase.

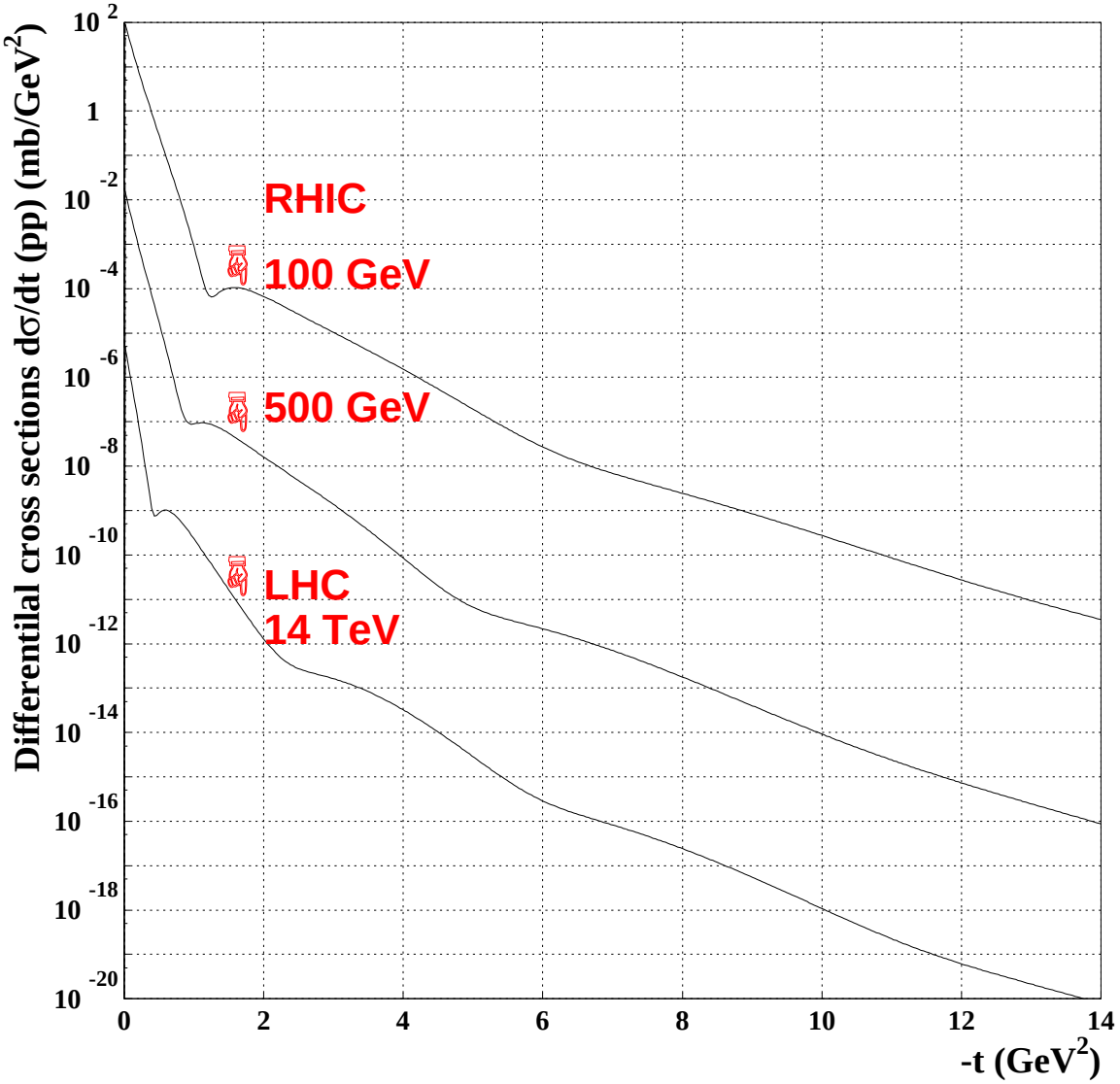

Figure 9: Prediction of the model for the pp scattering differential cross section at **RHIC** ($\sqrt{s} = 100,\ 500\ GeV$) and **LHC** ($\sqrt{s} = 14\ TeV$). A 10^{-4} factor between each successive set of data is omitted. The prediction for **RHIC** at the energy of $\sqrt{s} = 500\ GeV$ is multiplied by a factor of 10^{-4} and the prediction for **LHC** at the energy of $\sqrt{s} = 14\ TeV$ is multiplied by a factor of 10^{-8}.

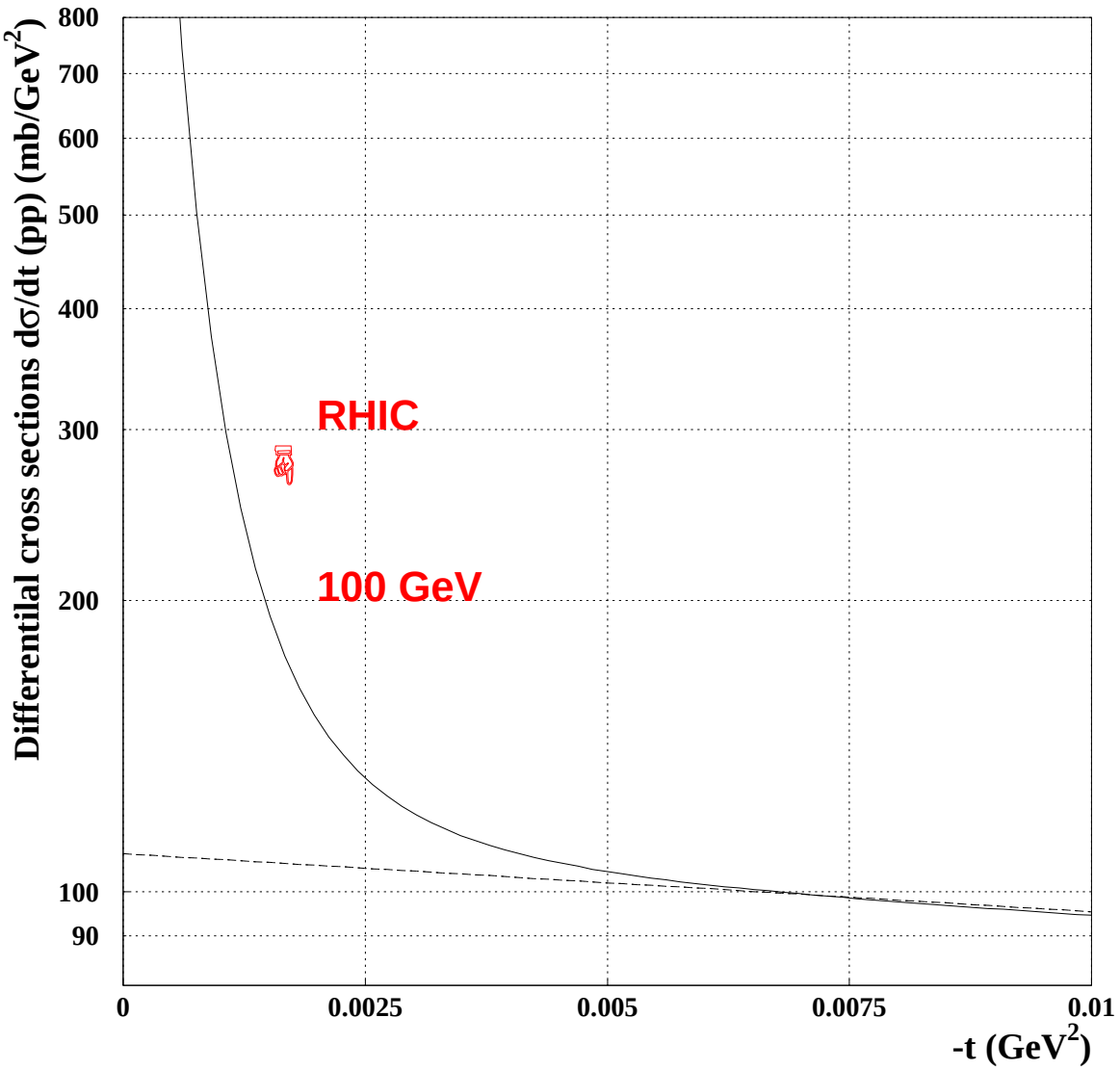

Figure 10: Prediction of the model for the pp scattering differential cross section at **RHIC** ($\sqrt{s} = 100\ GeV$). The solid line corresponds to full amplitude including the Coulombic one and the dashed line corresponds to the nuclear amplitude [1].

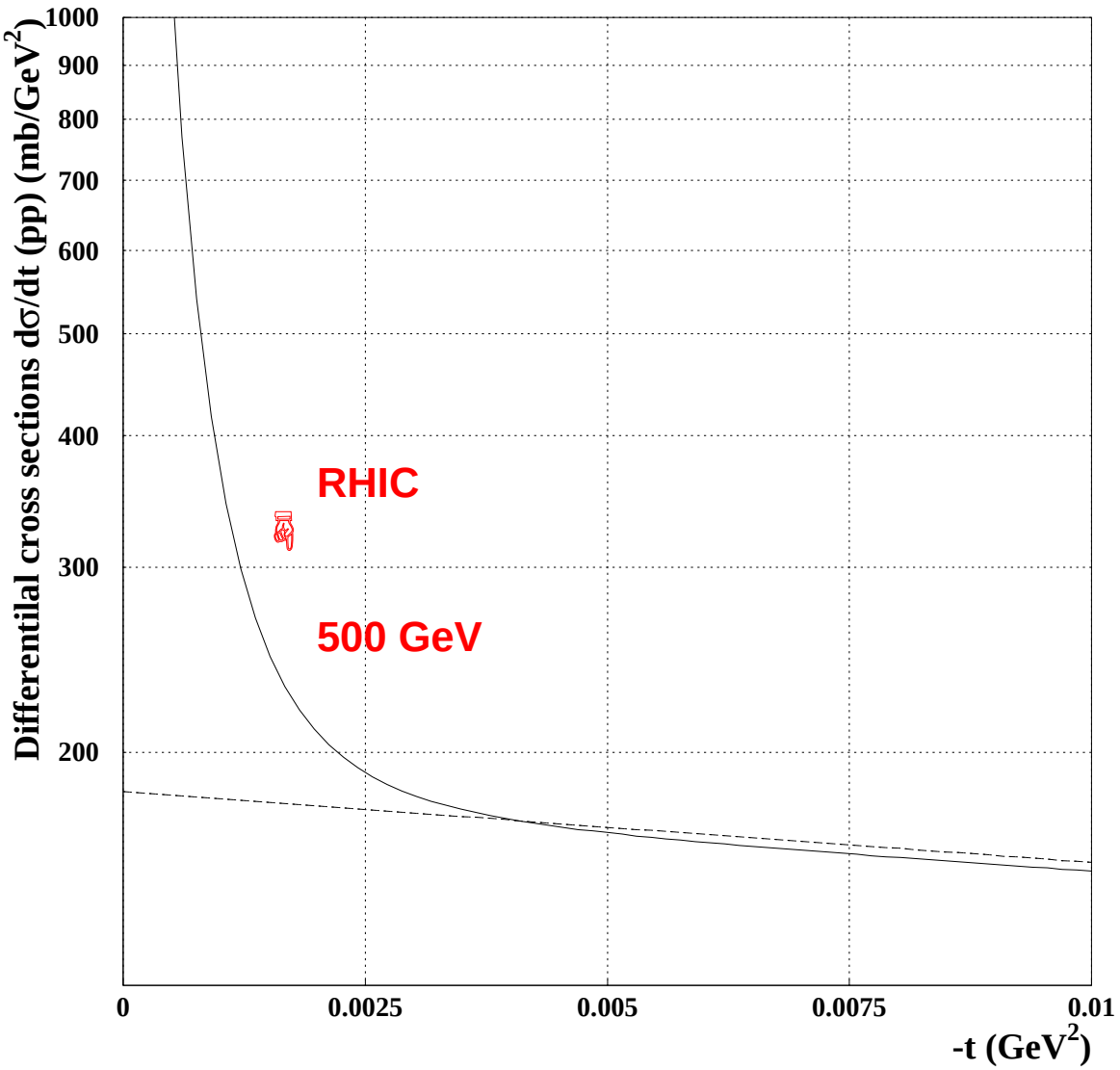

Figure 11: Prediction of the model for the pp scattering differential cross section at **RHIC** ($\sqrt{s} = 500\ GeV$). The solid line corresponds to full amplitude including the Coulombic one and the dashed line corresponds to the nuclear amplitude [1].

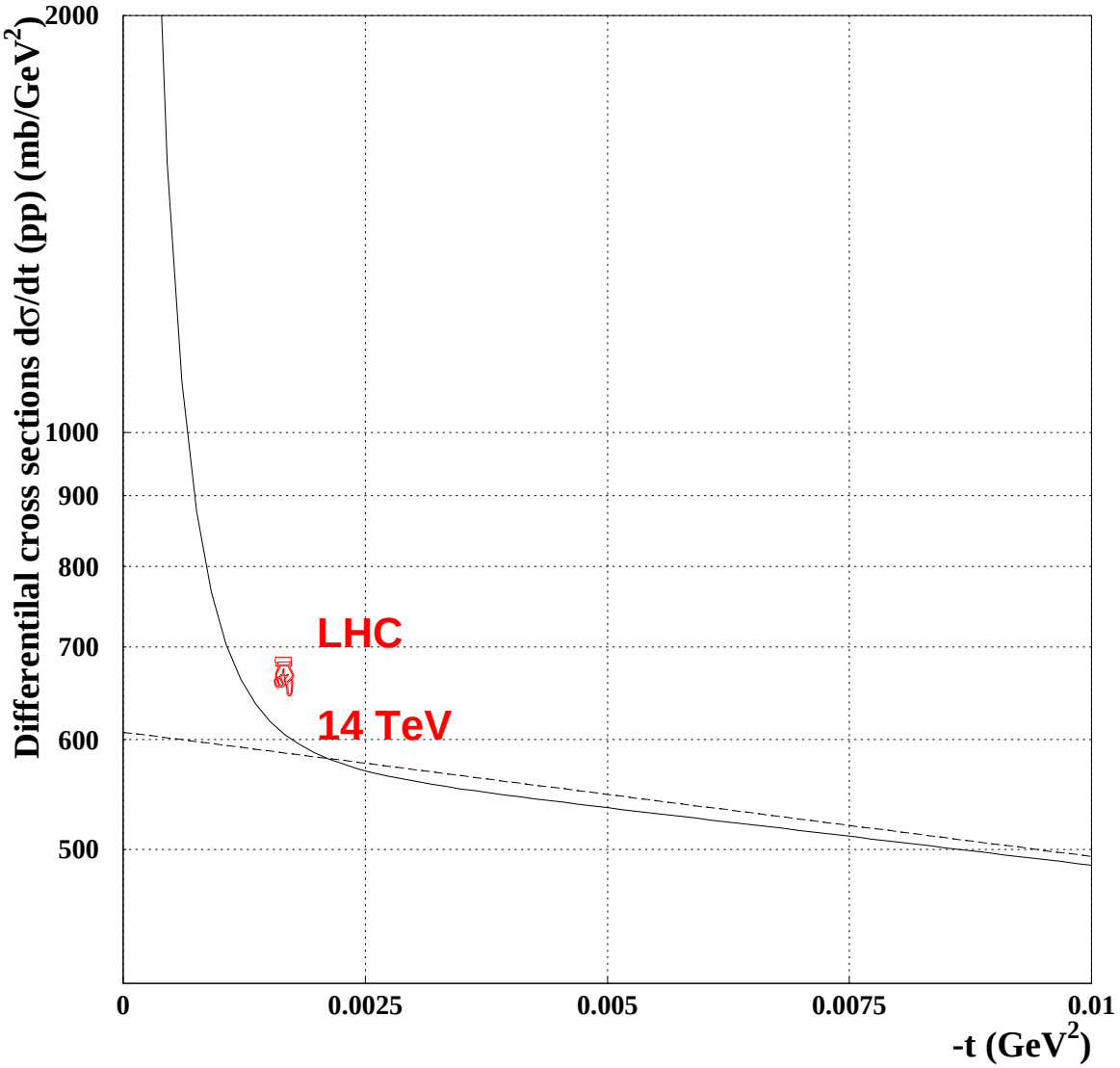

Figure 12: Prediction of the model for the pp scattering differential cross section at **LHC** ($\sqrt{s} = 14\ TeV$). The solid line corresponds to full amplitude including Coulombic one and the dashed line corresponds to the nuclear amplitude [1].

To show the influence of the interference between nucleon and Coulomb

amplitudes we show the ratio

$$R = \frac{\left| \frac{d\sigma}{dt} - \frac{d\sigma_{nucleon}}{dt} - \frac{d\sigma_{coulomb}}{dt} \right|}{\frac{d\sigma}{dt}}, \ [\%] \tag{21}$$

in figures 13 and 14 and we conlude that the interference term becomes negligible at **RHIC** and **LHC** energies at $t \sim -0.01\ GeV^2$ for **RHIC** and $t \sim -0.005\ GeV^2$ for **LHC**.

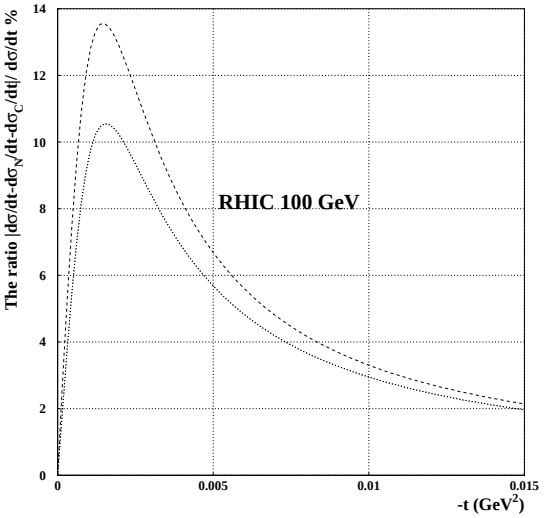

Figure 13: The interference term between hadron and Coulomb amplitudes for at the **RHIC** energy. The dashed line corresponds to the Coulomb phase calculated with the prescription of Selyugin [9] and the dotted line to the zero Coulomb phase.

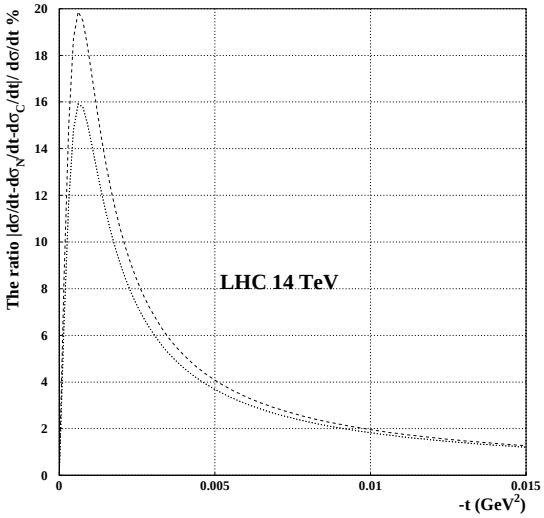

Figure 14: The interference term between hadron and Coulomb amplitudes at the **LHC** energy. The dashed line corresponds to the Coulomb phase calculated with the prescription of Selyugin [9] and the dotted line to the zero Coulomb phase.

Now let us return to the problem of extracting the ratio $\rho(s, t = 0)$ of the real to the imaginary parts of the scattering amplitude. A general theorem [14] shows that this ratio as a function of the momentum transfer could not have a constant sign in a strip $s_M < s < \infty$, $-T < t \leq 0$, for any s_M and $T > 0$. The method of extracting the ratio includes a simplification, the scattering amplitude is usually presented in the following form:

$$T(s,t) = \mp \frac{8\pi\alpha s}{|t|} f^2(|t|) + (i + \rho(s,0)) s\sigma_{tot} e^{Bt}(1 - i\alpha\Phi) \qquad (22)$$

where the ratio $\rho(s,t)$ is approximated by its value at $t = 0$. Should this simplification affect the measurement? The answer would be "yes" should the change of sign of ρ occurr close to the region of the maximum of the Coulomb nuclear interference.

In our particular model, the zero of the real part of the scattering amplitude goes to zero with the increase of energy, but remains far from the region of the maximum of the interference. For example, at LHC energies $\sqrt{s} = 14\ TeV$, the maximum occurs at $|t_{max}| \sim 10^{-3}\ GeV^2$ (fig.14) while the zero is at $|t_{zero}| \sim 0.16\ GeV^2$ (fig. 15, 16), so the situation is not too bad.

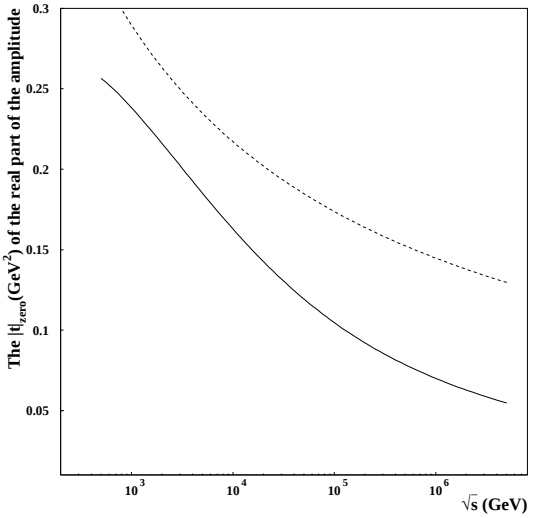

Figure 15: The position of the zero of the real part of the scattering amplitude in a three-component Pomeron model [1] (solid line) and in a "geometrical scaling" model $t_{zero} = -1/(\lambda \ln s)$, $\lambda = 0.25\ GeV^{-2}$ [14] (dashed line).

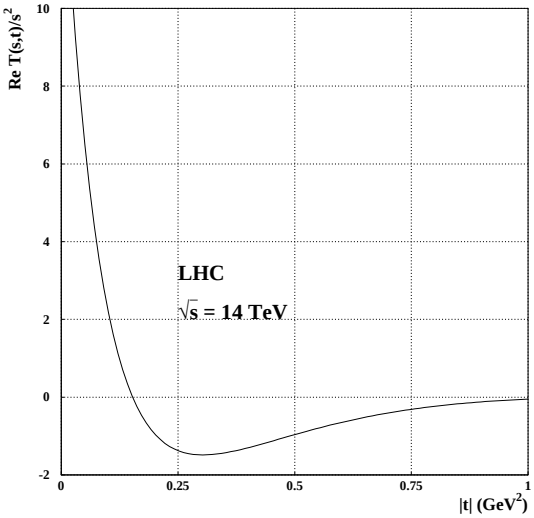

Figure 16: The real part of the scattering amplitude at the **LHC** energy in the model [1].

CONCLUSION

All the three choices of the Coulomb phase give good description of the existing data, though in terms of χ^2 per point the data "prefer" the phase calculated with the prescriptions of Cahn [3] (17) and Selyugin [9] (11). We conclude that such prescriptions are a good basis for the evaluation of the Coulombic contribution in the full scattering amplitude. We expect that similar conclusion would apply to an analysis repeated along the lines of [12] but we have not performed this analysis.

As we have seen, the addition of the nuclear amplitude (with parameters fitted from total and differential cross sections) and of the Coulomb one (with its proper phase) gives a total amplitude which reproduces quite well the data in the interference region without any additional parameters and with no need to refit existing ones.

This allows us to predict the **RHIC** Coulomb interference which requires the measurements to start from $|t| \leq 0.005\ GeV^2$ at the energy of $\sqrt{s} = 100\ GeV$ and from $|t| \leq 0.004\ GeV^2$ at the energy of $\sqrt{s} = 500\ GeV$. Likewise, **LHC** will be able to cover the Coulomb region if the measurement starts from $|t| \leq 0.001\ GeV^2$.

ACKNOWLEDGMENTS

We would like to thank E. Martynov and O. Selyugin for useful discussions.

References

[1] V.A. Petrov, A.V.Prokudin, *Eur.Phys.J.* C **23**, 135-143 (2002).

[2] G. B. West and D. R. Yennie, *Phys. Rev.* D **172**, 1413 (1968).

[3] R. Cahn, *Z. Phys.* C **15**, 253 (1982).

[4] H. Bethe, *Ann. Phys.* **3**, 190 (1958).

[5] J. Rix and R. M. Thaler, *Phys. Rev.* D **152**, 1357 (1966).

[6] M. M. Islam, *Phys. Rev.* D **162**, 1426 (1967).

[7] L. D. Soloviev, *JETP* **22**, 205 (1966).

[8] J. Rix and R. M. Thaler, *Phys. Rev.* D **172**, 1414 (1968).

[9] O. V. Selyugin, *Phys. Rev.* D **60**, 074028 (1999).

[10] P.Desgrolard, A.I.Lengyel, E.S.Martynov, *Nuovo Cimento* A **110**, 251-266 (1997).

[11] C. Bourelly, J. Soffer, Tai Tsun Wu, *Z. Phys.* C **37**, 369-375 (1988).

[12] B. Z. Kopeliovich and A. V. Tarasov, *Phys. Lett.* B **497**, 44 (2001).

[13] P. Desgrolard, M. Giffon, E. Martynov and E. Predazzi, *Eur.Phys.J.* C **16**, 499-511 (2000).

[14] A. Martin, *Phys. Lett.* B **404**, 137 (1997).